Published in final edited form as:
Am J Med Genet A. 2014 August ; 164(8): 2013–2019. doi:10.1002/ajmg.a.36606.

Two deletions overlapping a distant *FOXF1* enhancer unravel the role of lncRNA *LINC01081* in etiology of Alveolar Capillary Dysplasia with Misalignment of Pulmonary Veins

Przemyslaw Szafranski[1,*], **Avinash V. Dharmadhikari**[1,2], **Jennifer A. Wambach**[3], **Chris T. Towe**[3], **Frances V. White**[4], **R. Mark Grady**[3], **Pirooz Eghtesady**[5], **F. Sessions Cole**[3], **Gail Deutsch**[6], **Partha Sen**[7], and **Pawel Stankiewicz**[1,2]

[1]Department of Molecular and Human Genetics, Baylor College of Medicine, Houston, TX, USA

[2]Interdepartmental Program in Translational Biology and Molecular Medicine, Baylor College of Medicine, Houston, TX, USA

[3]Edward Mallinckrodt Department of Pediatrics

[4]Department of Pathology and Immunology

[5]Department of Surgery, Washington University School of Medicine, St. Louis, MO, USA

[6]Department of Pathology, Seattle Children's Hospital, Seattle, WA

[7]Department of Pediatrics – Newborn, Baylor College of Medicine, Houston, TX, USA

Abstract

Position effects due to disruption of distant *cis*-regulatory regions have been reported for over 40 human gene loci; however, the underlying mechanisms of long-range gene regulation remain largely unknown. We report two patients with Alveolar Capillary Dysplasia with Misalignment of Pulmonary Veins (ACDMPV) caused by overlapping genomic deletions that included a distant *FOXF1* transcriptional enhancer mapping 0.3 Mb upstream to *FOXF1* on 16q24.1. In one patient with atypical late-onset ACDMPV, a ~ 1.5 Mb deletion removed the proximal 43% of this enhancer, leaving the lung-specific long non-coding RNA (lncRNA) gene *LINC01081* intact. In the second patient with severe neonatal-onset ACDMPV, an overlapping ~ 194 kb deletion disrupted *LINC01081*. Both deletions arose *de novo* on maternal copy of the chromosome 16, supporting the notion that *FOXF1* is paternally imprinted in the human lungs. RNAi-mediated knock-down of *LINC01081* in normal fetal lung fibroblasts showed that this lncRNA positively regulates *FOXF1* transcript level, further indicating that decrease in *LINC01081* expression can contribute to development of ACDMPV.

Keywords

ACDMPV; gene regulation; position effect; long non-coding RNA; genomic imprinting

[*]**Correspondence to:** Dr. Przemyslaw Szafranski, Dept. of Molecular and Human Genetics, Baylor College of Medicine, One Baylor Plaza, Rm R851C, Houston, TX 77030, USA. Tel.: 713 798 5375, Fax: 713798 7418, pszafran@bcm.edu.

Supporting Information
Additional supporting information may be found in the online version of this article at the publisher's web-site.

Introduction

Alveolar Capillary Dysplasia with Misalignment of Pulmonary Veins (ACDMPV) (OMIM 265380) is a rare, lethal disorder of the lungs. Affected patients typically present with severe respiratory failure and refractory pulmonary hypertension within a few hours after birth and die in the first month of life, although rare late-onset presentations have been reported [Abdallah et al., 1993; Licht et al., 2004; Shankar et al., 2006; Ahmed et al., 2008]. Histopathologically, ACDMPV is characterized by malposition of pulmonary veins adjacent to small pulmonary arteries, medial thickening of small pulmonary arteries, deficient lobular development, a paucity of alveolar wall capillaries, and occasional lymphangiectasis [Langston 1991]. The majority of patients with ACDMPV also have extra-pulmonary anomalies of the gastrointestinal, cardiovascular, and genitourinary systems [Sen et al., 2004; Bishop et al., 2011].

Heterozygous point mutations or genomic deletions of *FOXF1* (MIM 601089) have been reported in most patients with ACDMPV [Stankiewicz et al., 2009; Sen et al., 2013a,b; Szafranski et al., 2013a]. Recently, we have defined a ~ 75 kb differentially methylated and evolutionarily conserved *cis*-regulatory region mapping to a protein-coding gene desert ~ 257 kb upstream to *FOXF1* and functioning as its tissue-specific enhancer [Szafranski et al., 2013b]. This region harbors, among others, genes for fetal lung-enriched long non-protein coding RNAs (lncRNAs), transcription factor GLI2-binding sites, and the differentially-methylated CpG island, likely contributing to the paternal genomic imprinting of the *FOXF1* in the human lungs [Sen et al., 2013a,b; Szafranski et al., 2013a].

lncRNAs are the least understood elements of the *FOXF1* distant enhancer. These RNAs are broadly classified as 5′-capped and polyadenylated transcripts longer than 100-200 nucleotides (nt) (as opposed to 21-35-nt miRNAs and other small RNAs), and exhibiting very limited protein-coding potential [Yang et al., 2014]. More than 1/3 of the already studied lncRNAs associate with chromatin modifying complexes and target them to specific genomic regions [Khalil et al., 2009]. Others function as decoys for transcription regulators and miRNAs, as suppliers of transcription factor and repressor complexes for promoters, or can be directly involved in posttranscriptional regulation of mRNA processing, and translation [Yang et al., 2014].

Here, we show that partial deletion of the distant *FOXF1* enhancer that leaves the lncRNA *LINC01081* intact, was associated with a late-onset ACDMPV phenotype, whereas an overlapping deletion that disrupted the *LINC01081* gene resulted in a neonatal-onset, classic ACDMPV phenotype. We verified the role of *LINC01081* in regulation of the *FOXF1* expression and etiology of ACDMPV by RNAi-based *FOXF1* knock-down in fetal lung fibroblasts.

Material and Methods

DNA and RNA isolation, DNA sequencing and sequence analysis

Blood and lung samples were obtained after informed consents. DNA was extracted from peripheral blood, and RNA was extracted from FFPE ACDMPV lung tissue, frozen normal lung tissue, and normal human fetal lung fibroblasts MRC-5 and IMR-90 (ATCC) as described [Szafranski et al. 2013a,b]. PCR products were directly sequenced by the Sanger method. Reference sequences were downloaded from the UCSC Genome Browser (NCBI build 37/hg19, http://genome.ucsc.edu). Sequences were assembled using Sequencher v4.8 (GeneCodes).

Array CGH and deletion analysis

Genomic copy-number variants (CNVs) were analyzed using array CGH with custom-designed 16q24.1 region-specific 3x720K microarrays (Roche NimbleGen) (patient 99.3) and 4x180K microarrays (Agilent) (patient 111.3) according to manufacturer's protocols. Amplification of a junction fragment for sequencing was performed using LA Taq polymerase (TaKaRa Bio USA) as described [Szafranski et al. 2013a,b]. Parental origin of the deletion was determined following identification of an informative SNP and a microsatellite polymorphism in parental and patient's chromosomes.

Real time quantitative PCR analysis of the FOXF1 transcript

RNA samples from control and ACDMPV lungs and from cultured normal fetal lung fibroblasts were reverse-transcribed using High Capacity cDNA Reverse Transcription Kit (Applied Biosystems). TaqMan primers and probes were synthesized by Applied Biosystems. Primers for *FOXF1* were: 5′-CGAGCTGCAAGGCATCCCGCGGTAT-3′ and 5′-CAAGAGGAAGAGAGAGACCCTCACT-3′. *FOXF1* transcript levels were normalized to *GAPDH*. qPCR was repeated four times using TaqMan Universal PCR Master Mix (Applied Biosystems). qPCR conditions included 40 cycles of 95°C for 15 s and 60°C for 1 min. For relative quantification of the *FOXF1* transcript, the comparative ΔC_T method was used. Normal fetal lung was designated as a calibrator sample.

siRNA knock-down of lncRNAs

Knock-down experiments with RNAi were performed using two custom-designed (Ambion) Silencer Select siRNA doublets per knock-down (Table S1 – see supporting information online). IMR-90 cells were maintained in the Eagle's minimum essential medium (EMEM) supplemented with 2 mM L-glutamine and 10% FBS (ATCC). For siRNA transfection, cells were treated with Lipofectamine RNAiMAX (Invitrogen) according to the manufacturer's protocol. 4.5 μl of Lipofectamine per well in 12-well plate format was applied. The final concentration of each siRNA was 15 nM. RNA was prepared from cultured cells 48 hrs after transfection.

Clinical Report

Patient 1

Patient 1 (99.3) was a full term 4.57 kg female infant born to a 29-year-old gravida 2 para 2 mother, whose pregnancy was complicated by type I diabetes. Shortly after birth, the infant developed respiratory distress with tachypnea and retractions. Over the next six months, she had marginal weight gain and persistent subcostal retractions. At seven months of age she developed acute respiratory distress and fever while vacationing with her family at high altitude. Her examination was significant for severe subcostal retractions, hypoxemia (oxygen saturations of 86-93% while breathing room air), and tachypnea. Chest radiograph demonstrated scattered interstitial opacities (Fig. 1A) and her chest lung CT showed diffuse, bilateral ground-glass infiltrates with extensive septal line thickening and scattered areas of mosaic attenuation. Her echocardiogram demonstrated evidence of significant pulmonary hypertension, and she was commenced on inhaled nitric oxide and oral sildenafil. A lung biopsy showed misalignment of the pulmonary veins, diffuse smooth muscle hyperplasia of arteries and arterioles, and focal areas of centrally located capillaries within widened alveolar septa. She clinically stabilized and did relatively well until 14 months of age when she developed severe hypoxic respiratory failure due to viral respiratory infection and required extracorporeal membrane oxygenation (ECMO). She underwent orthotopic bilateral lung transplantation at 15 months of age. Her explanted lung showed scattered misaligned veins within bronchovascular bundles in all lobes, central placement of capillaries within widened alveolar septa in peripheral areas of all lobes, diffuse medial wall thickening of arteries and arterioles, and marked lymphangiectasia in interlobular septa and around bronchovascular bundles (Fig. 1B, C).

Patient 2

Patient 2 (111.3) was a full-term male infant presenting with cyanosis and hypoxemia (50%) at a few hours of life and required intubation. Echocardiogram demonstrated severe pulmonary hypertension with exclusive right to left shunting through his patent ductus arteriosus and dilated right ventricle with depressed function. He had no clinical response to inhaled nitric oxide and trepostinil and was placed on ECMO for refractory respiratory failure. He continued to demonstrate severe pulmonary hypertension. Lung biopsy at 11 days of age confirmed the clinical suspicion of ACDMPV (Fig. 1D). Due to the poor prognosis, ECMO was discontinued, and he died at 13 days of life. Lungs at autopsy demonstrated the features of ACDMPV with diffuse misalignment of pulmonary veins.

Results

Histopathological analysis of lung biopsy and explant in patient 99.3 showed characteristic findings of ACDMPV (Fig. 1B, C). While this patient had persistent respiratory symptoms that began in the newborn period, she did not develop respiratory failure until after a year of life, consistent with atypical ACDMPV. Her late presentation correlated with pathological features of the explanted lung, which demonstrated scattered misaligned veins. Lung biopsy in patient 111.3 showed the typical ACDMPV features with diffusely misaligned veins (Fig. 1D).

In both cases, DNA sequencing did not find any evidence of point mutation in *FOXF1*. Array CGH analyses revealed two overlapping deletions on 16q24.1 leaving *FOXF1* intact: a ~ 1.5 Mb deletion mapping ~ 306 kb upstream to *FOXF1* in patient 99.3 and a ~ 194 kb deletion located ~ 272 kb upstream to *FOXF1* in patient 111.3 (Fig. 2A). In patient 99.3 with an atypical ACDMPV presentation, the deletion removed 26 kb of the proximal portion (chr16:86,212,040-86,238,601/86,238,621) of the ~ 75 kb *FOXF1* enhancer region (chr16:86,212,040-86,287,054), but left the lung-specific lncRNA gene *LINC01081* intact (Fig. 2B). In patient 111.3 with severe ACDMPV, the deletion extended to chr16:86,271,915/86,271,919, and disrupted *LINC01081*, thus narrowing the enhancer region to ~ 60 kb (chr16:86,212,040-86,271,915/86,271,919) (Fig. 2B).

Real-time qPCR analysis of RNA isolated from the FFPE lung tissue from patient 99.3 demonstrated a significant (70%) reduction of *FOXF1* expression when compared with that in normal lungs (Fig. 3). However, since only a single FFPE specimen was available for analysis, we could not estimate mean expression of *FOXF1* in her lungs for comparison with *FOXF1* transcript levels in a severe ACDMPV cases (Szafranski et al., 2013a).

To infer the molecular mechanisms of deletion formation and to assess recurrence risk, we sequenced the breakpoints of both deletions. In patient 99.3, both deletion breakpoints mapped within the *Alu* repetitive elements; the proximal breakpoint mapped within *Alu*Sc8 between 84,764,627 and 84,764,647, and the distal breakpoint within *Alu*Y between 86,238,601 and 86,238,621 (Fig. 4A). The proximal breakpoint of the deletion in patient 111.3 mapped within LTR ERVL, between 86,077,954 and 86,077,958 and the distal breakpoint mapped within LINE L1 element, between 86,271,915 and 86,271,919 (Fig. 4A). In both deletions, the breakpoints were associated with the presence of 19 bp (99.3) and 3 bp (111.3) microhomologies, suggesting they might have arisen by a template switching replicative mechanism such as fork stalling and template switching (FoSTeS) or microhomology-mediated break-induced replication (MMBIR) [Lee et al., 2007; Hastings et al., 2009]. Of interest, three of the four breakpoints were adjacent to DNA regions with locally increased GC content (data not shown).

Consistent with the accumulating evidence that suggests partial paternal imprinting of the *FOXF1* locus [Stankiewicz et al. 2009; Sen et al., 2013b; Szafranski et al., 2013a,b], we found that both deletions arose *de novo* on the maternal chromosome 16 (Fig. 4B). We did not find any evidence for low-level somatic mosaicism in either of the maternal DNA samples using PCR for patient-specific junction fragments (Fig. 4C).

To experimentally verify the involvement of *LINC01081* in regulation of *FOXF1* expression and etiology of ACDMPV, we reduced the levels of lncRNAs *LINC01081* and *TCONS_00024781* (a lung-enriched stand-alone lncRNA encoded in chr16q24.1, but not within any of the deleted regions) using RNAi in normal fetal lung fibroblasts, and quantified *FOXF1* expression by RT qPCR. We found that targeting *LINC01081* with two different pairs of siRNAs reduced *FOXF1* transcript levels by 14 and 20%, whereas decreasing the expression of *TCONS_00024781* did not affect the *FOXF1* expression (Fig. 5). Thus, we conclude that *LINC01081* positively and specifically regulates *FOXF1*

expression. The discordance in phenotypes between our patients suggests that regulation of *FOXF1* expression by *LINC01081* contributes to onset of ACDMPV symptoms.

Discussion

Recently, we characterized an ~ 75 kb *FOXF1* transcriptional enhancer defined by nine overlapping deletions. It maps ~ 257 kb upstream to *FOXF1*, includes two conserved segments that exhibit high regulatory potential, and encodes differentially-spliced lung-specific lncRNAs [Szafranski et al., 2013]. Deletion of the entire enhancer or its mislocalization (*e.g.* due to balanced inversion) resulted in the neonatal onset classic ACDMPV phenotype [Stankiewicz et al., 2009; Szafranski et al., 2013a; Parris et al., 2013]. Genotype-phenotype correlations in patient (99.3) with atypical ACDMPV and in patient (111.3) with severe early-onset ACDMPV enabled us to further narrow this enhancer region. Array CGH analyses revealed overlapping deletions at chr16q24.1 that removed 35% (patient 99.3) and 80% (patient 111.3) of the ~ 75 kb *FOXF1* enhancer region.

The vast majority of children with ACDMPV die, like patient 111.3, within the first month of life; longer survivals and later presentations have been rarely reported [Abdallah et al., 1993; Licht et al., 2004; Shankar et al., 2006; Ahmed et al., 2008]. Patient 99.3 had mild respiratory symptoms at birth and survived 15 months before undergoing lung transplantation and was one of the oldest known patient with atypical presentation of ACDMPV. Whereas her lung biopsy and explant showed the hallmark features of ACDMPV, there was non-uniform distribution of misaligned veins in the bronchovascular bundles compared to that typically observed in patients with severe full ACDMPV phenotype.

Correlation analysis of the deletions and their associated lung phenotypes in our two patients indicated that: (i) removal of one of the two segments of this enhancer region, Segment 1, that contains GLI2-binding sites, partially overlapping differentially methylated CpG island, and a lncRNA gene *LINC01082*, results in a milder atypical form of ACDMPV with focal pulmonary vein misalignment, and that (ii) decrease of the lung-specific lncRNA *LINC01081*, partially encoded by the Segment 2 of the enhancer and disrupted in patient 111.3 (in addition to the loss of the Segment 1) contributes to severity of ACDMPV likely by decreasing *FOXF1* expression. Late onset of ACDMPV and scattered interstitial opacities in the lungs in patient 1 could be also explained by lung somatic mosaicism that was not detectable in the blood. Using RNAi, we decreased the levels of *LINC01081* in normal fetal lung fibroblasts, demonstrating that indeed *LINC01081* regulates expression of *FOXF1*.

The molecular mechanisms of positive regulation of gene expression by lncRNAs are only starting to emerge [Tsai et al., 2010; Ørom et al., 2014]. We speculate that *LINC01081* may control *FOXF1* expression through modification of chromatin architecture around the *FOXF1* promoter, by supplying the promoter with transcription factors, or by providing the decoy targets for miRNAs or transcription inhibitors. Using qPCR, we also showed that deletion of Segment 1 in patient 99.3 correlates with decrease of *FOXF1* transcript, independently indicating that this enhancer indeed controls expression of *FOXF1 in vivo*. It

would be interesting to study the phenotypic effects of knock-down of the other lincRNA *LINC01082*.

Of interest, both *de novo* deletions arose on maternal copy of chromosome 16, similarly to other 16 previously analyzed *FOXF1* locus deletions in patients with ACDMPV, further supporting the notion that *FOXF1* is paternally imprinted in the human lungs, although incompletely [Stankiewicz et al. 2009; Szafranski et al. 2103a; Sen et al. 2013a].

In summary, (i) we narrowed the regulatory region located ~ 272 kb upstream to *FOXF1* to ~ 60 kb and showed that its loss correlated with *FOXF1* expression *in vivo*, (ii) demonstrated that lncRNA *LINC01081*, encoded in the distal portion of this enhancer (Segment 2), positively regulated *FOXF1* transcript level and its disruption can contribute to the development of the classic neonatal-onset ACDMPV phenotype, and (iii) provide data indicating that the removal of the proximal portion of the enhancer (Segment 1), containing GLI2-binding sites and lncRNA *LINC01082*, but leaving *LINC01081* intact, can result in atypical ACDMPV.

Supplementary Material

Refer to Web version on PubMed Central for supplementary material.

Acknowledgments

This work was supported by NIH grant 1RO1HL101975-01 to P. Stankiewicz, R01 HL065174 and R01 HL082747 to F.S. Cole, K08 HL105891 to J.A. Wambach, and NORD grants to P. Szafranski, and P. Sen.

References

Abdallah HI, Karmazin N, Marks LA. Late presentation of misalignment of lung vessels with alveolar capillary dysplasia. Crit Care Med. 1993; 21:628–630. [PubMed: 8472585]

Ahmed S, Ackerman V, Faught P, Langston C. Profound hypoxemia and pulmonary hypertension in a 7-month-old infant: late presentation of alveolar capillary dysplasia. Pediatr Crit Care Med. 2008; 9:e43–e46. [PubMed: 18997591]

Bishop NB, Stankiewicz P, Steinhorn RH. Alveolar capillary dysplasia. Am J Respir Crit Care Med. 2011; 184:172–179. [PubMed: 21471096]

Hastings PJ, Lupski JR, Rosenberg SM, Ira G. Mechanisms of change in gene copy number. Nat Rev Genet. 2009; 10:551–564. [PubMed: 19597530]

Khalil AM, Guttman M, Huarte M, Garber M, Raj A, Rivea Morales D, Thomas K, Presser A, Bernstein BE, van Oudenaarden A, Regev A, Lander ES, Rinn JL. Many human large intergenic noncoding RNAs associate with chromatin-modifying complexes and affect gene expression. Proc Natl Acad Sci USA. 2009; 106:11667–11672. [PubMed: 19571010]

Langston C. Misalignment of pulmonary veins and alveolar capillary dysplasia. Pediatr Pathol. 1991; 11:163–170. [PubMed: 2014189]

Lee JA, Carvalho CM, Lupski JR. A DNA replication mechanism for generating nonrecurrent rearrangements associated with genomic disorders. Cell. 2007; 131:1235–1247. [PubMed: 18160035]

Licht C, Schickendantz S, Sreeram N, Arnold G, Rossi R, Vierzig A, Mennicken U, Roth B. Prolonged survival in alveolar capillary dysplasia syndrome. Eur J Pediatr. 2004; 163:181–182. [PubMed: 14677063]

Ørom UA, Derrien T, Beringer M, Gumireddy K, Gardini A, Bussotti G, Lai F, Zytnicki M, Notredame C, Huang Q, Guigo R, Shiekhattar R. Long noncoding RNAs with enhancer-like function in human cells. Cell. 2010; 143:46–58. [PubMed: 20887892]

Parris T, Nik AM, Kotecha S, Langston C, Helou K, Platt C, Carlsson P. Inversion upstream of *FOXF1* in a case of lethal alveolar capillary dysplasia with misalignment of pulmonary veins. Am J Med Genet A. 2013; 161A:764–770. [PubMed: 23444129]

Sen P, Gerychova R, Janku P, Jezova M, Valaskova I, Navarro C, Silva I, Langston C, Welty S, Belmont J, Stankiewicz P. A familial case of alveolar capillary dysplasia with misalignment of pulmonary veins supports paternal imprinting of *FOXF1* in human. Eur J Hum Genet. 2013b; 21:474–477. [PubMed: 22990143]

Sen P, Thakur N, Stockton DW, Langston C, Bejjani BA. Expanding the phenotype of alveolar capillary dysplasia (ACD). J Pediatr. 2004; 145:646–651. [PubMed: 15520767]

Sen P, Yang Y, Navarro C, Silva I, Szafranski P, Kolodziejska KE, Dharmadhikari AV, Mostafa H, Kozakewich H, Kearney D, Cahill JB, Whitt M, Bilic M, Margraf L, Charles A, Goldblatt J, Gibson K, Lantz PE, Garvin AJ, Petty J, Kiblawi Z, Zuppan C, McConkie-Rosell A, McDonald MT, Peterson-Carmichael SL, Gaede JT, Shivanna B, Schady D, Friedlich PS, Hays SR, Palafoll IV, Siebers-Renelt U, Bohring A, Finn LS, Siebert JR, Galambos C, Nguyen L, Riley M, Chassaing N, Vigouroux A, Rocha G, Fernandes S, Brumbaugh J, Roberts K, Ho-Ming L, Lo IF, Lam S, Gerychova R, Jezova M, Valaskova I, Fellmann F, Afshar K, Giannoni E, Muhlethaler V, Liang J, Beckmann JS, Lioy J, Deshmukh H, Srinivasan L, Swarr DT, Sloman M, Shaw-Smith C, van Loon RL, Hagman C, Sznajer Y, Barrea C, Galant C, Detaille T, Wambach JA, Cole FS, Hamvas A, Prince LS, Diderich KE, Brooks AS, Verdijk RM, Ravindranathan H, Sugo E, Mowat D, Baker ML, Langston C, Welty S, Stankiewicz P. Novel *FOXF1* mutations in sporadic and familial cases of Alveolar Capillary Dysplasia with Misaligned Pulmonary Veins imply a role for its DNA binding domain. Hum Mutat. 2013a; 34:801–811. [PubMed: 23505205]

Shankar V, Haque A, Johnson J, Pietsch J. Late presentation of alveolar capillary dysplasia in an infant. Pediatr Crit Care Med. 2006; 7:177–179. [PubMed: 16474258]

Stankiewicz P, Sen P, Bhatt SS, Storer M, Xia Z, Bejjani BA, Ou Z, Wiszniewska J, Driscoll DJ, Maisenbacher MK, Bolivar J, Bauer M, Zackai EH, McDonald-McGinn D, Nowaczyk MM, Murray M, Hustead V, Mascotti K, Schultz R, Hallam L, McRae D, Nicholson AG, Newbury R, Durham-O'Donnell J, Knight G, Kini U, Shaikh TH, Martin V, Tyreman M, Simonic I, Willatt L, Paterson J, Mehta S, Rajan D, Fitzgerald T, Gribble S, Prigmore E, Patel A, Shaffer LG, Carter NP, Cheung SW, Langston C, Shaw-Smith C. Genomic and genic deletions of the FOX gene cluster on 16q24.1 and inactivating mutations of *FOXF1* cause alveolar capillary dysplasia and other malformations. Am J Hum Genet. 2009; 84:780–791. [PubMed: 19500772]

Szafranski P, Yang Y, Nelson MU, Bizzarro MJ, Morotti RA, Langston C, Stankiewicz P. Novel *FOXF1* deep intronic deletion causes lethal lung developmental disorder Alveolar Capillary Dysplasia with Misalignment of Pulmonary Veins. Hum Mutat. 2013a; 34:1467–1471. [PubMed: 23943206]

Szafranski P, Dharmadhikari AV, Brosens E, Storer M, Xia Z, Bejjani BA, Ou Z, Wiszniewska J, Driscoll DJ, Maisenbacher MK, Bolivar J, Bauer M, Zackai EH, McDonald-McGinn D, Nowaczyk MM, Murray M, Hustead V, Mascotti K, Schultz R, Hallam L, McRae D, Nicholson AG, Newbury R, Durham-O'Donnell J, Knight G, Kini U, Shaikh TH, Martin V, Tyreman M, Simonic I, Willatt L, Paterson J, Mehta S, Rajan D, Fitzgerald T, Gribble S, Prigmore E, Patel A, Shaffer LG, Carter NP, Cheung SW, Langston C, Shaw-Smith C. Small noncoding differentially methylated copy-number variants, including lncRNA genes, cause a lethal lung developmental disorder. Genome Res. 2013b; 23:23–33. [PubMed: 23034409]

Tsai MC, Manor O, Wan Y, Mosammaparast N, Wang JK, Lan F, Shi Y, Segal E, Chang HY. Long noncoding RNA as modular scaffold of histone modification complexes. Science. 2010; 329:689–693. [PubMed: 20616235]

Yang L, Froberg JE, Lee JT. Long noncoding RNAs: fresh perspectives into the RNA world. Trends Biochem Sci. 2014; 39:35–43. [PubMed: 24290031]

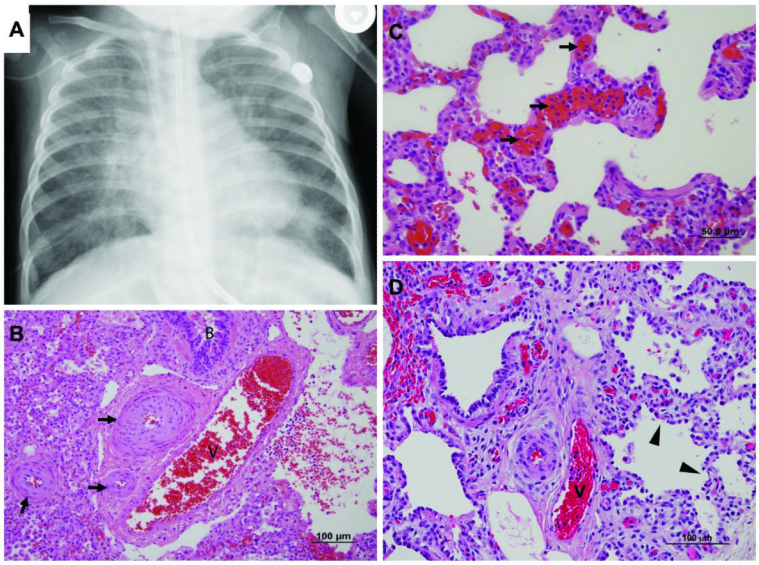

Figure 1.

ACDMPV lung pathology. (**A**) Chest radiograph showing scattered interstitial opacities in the case 99.3 lungs. (**B-D**) Histopathology of the lungs of cases 99.3 and 111.3. Sections of FFPE lung tissue were stained with hematoxylin and eosin. (**B**, **C**) Morphological changes characteristic for ACDMPV in the lung explant of patient 99.3 include increased medial smooth muscle in small pulmonary arteries (black arrows in panel B) and malposition of pulmonary veins (V identifies vein) adjacent to small pulmonary arteries in bronchovascular bundles (B identifies bronchioles). In addition, alveolar septa are widened with centrally-placed dilated and congested capillaries (black arrows in panel C). (**D**) The lung biopsy in case 111.3 demonstrates malposition of the veins (V) adjacent to pulmonary arteries, which show marked medial hypertrophy. Alveoli are simplified with poor approximation of capillaries to the alveolar space (arrowheads).

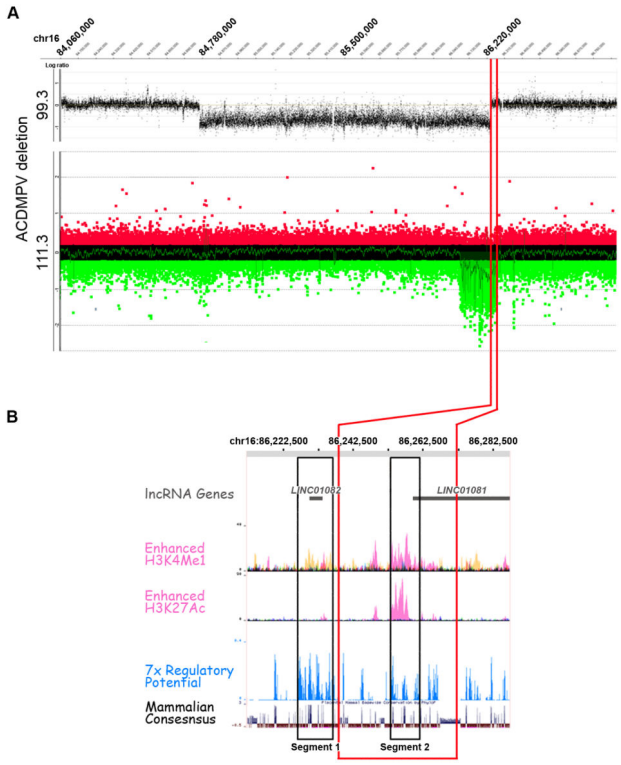

Figure 2.

16q24.1 deletion analysis. (**A**) Array CGH plots showing the ~ 1.5 Mb and ~ 194 kb deletions in 16q24.1 mapping ~ 306 kb and ~ 272 kb upstream to *FOXF1* in patients 99.3 and 111.3, respectively. (**B**) Selected genomic features of the *FOXF1* distant ~ 60 kb enhancer region (chr16:86,212,040-86,271,915/86,271,919) depicted using UCSC Genome Browser. Segment 1 and Segment 2 (black rectangles), harboring, among others, GLI2 transcription factor binding sites and genes for lung-enriched lncRNAs, are shown. H3K4Me1 and H3K27Ac are histone marks associated with enhancers and opened chromatin structure, respectively. The difference between the two deletions within the *FOXF1* enhancer is framed in red.

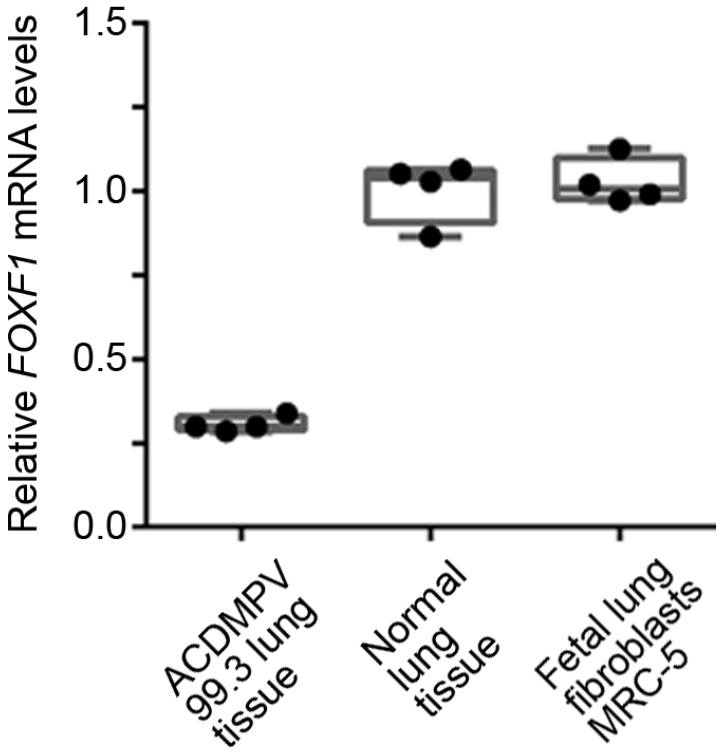

Figure 3.

Comparative RT qPCR analysis of the *FOXF1* mRNA levels in lung tissues of the ACDMPV case 99.3, normal individual, and normal human fetal lung fibroblasts MRC-5 (Kruskal-Wallis ANOVA test: P=0.013; Mann-Whitney test comparing ACDMPV lungs with normal fetal lungs or cultured normal lung fibroblasts: P=0.029).

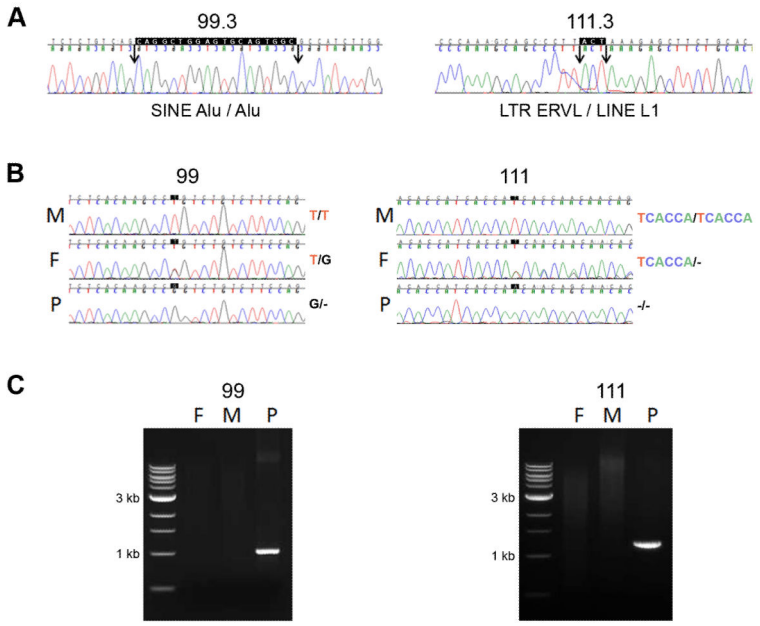

Figure 4.

Deletion breakpoints (P, M, and F depict proband, mother, and father, respectively). Chromatograms show (**A**) DNA sequences of the deletion junctions, including 19 bp and 3 bp microhomologies (highlighted black) and location of deletion breakpoints (arrows and the region between them), and (**B**) single-nucleotide and microsatellite polymorphisms indicating that both deletions originated on the maternal chromosome. (**C**) PCR amplification of proband's and parental DNA samples, using primers flanking the deletion junction, indicating that the deletion arose *de novo* in the proband.

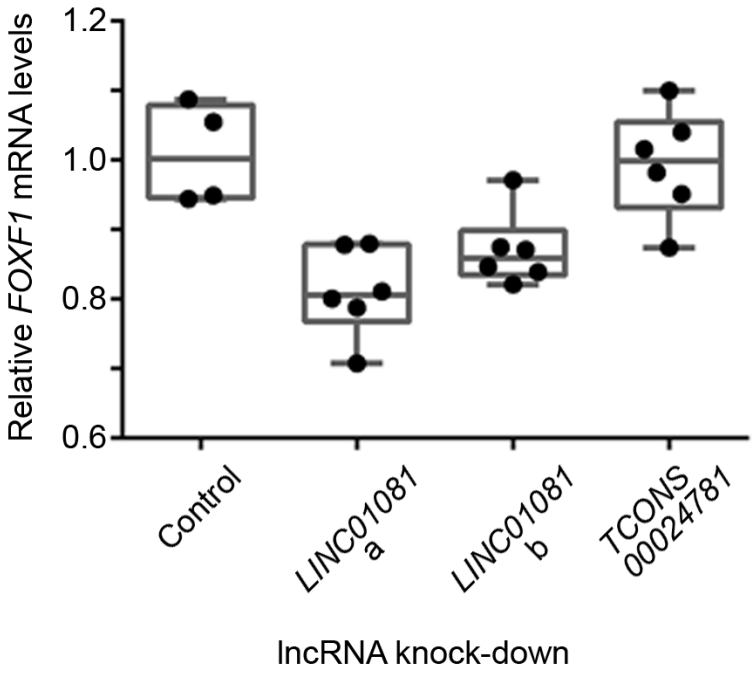

Figure 5.

Depletion of lncRNA *LINC01081* by RNAi in the normal human fetal lung fibroblasts, IMR-90, decreases *FOXF1* transcript level (Kruskal-Wallis ANOVA test: *P*=0.005, Mann-Whitney test comparing cells with and without knock-downed lncRNA: *P*=0.010). (a) and (b) depict use of two different pairs of siRNAs to knock-down *LINC01081* (Suppl. Table S1).